Rev. Roum. Sci. Techn.– Électrotechn. et Énerg.
Vol. **65**, *1-2*, pp. 109–115, Bucarest, 2020

ANALYTICAL DESIGN OF FRACTIONAL ORDER PROPORTIONAL-INTEGRAL CONTROLLER FOR ENHANCED POWER CONTROL OF DOUBLY-FED INDUCTION GENERATOR

SAMIR METATLA[1,2], SAID MEKHTOUB[1], ALI NESBA[3], ILHAMI COLAK[4], M'HAMED OUADAH[1,5]

Key words: Analytical design, Frequency specifications, Proportional integral (PI) controller, Fractional order, Integer order, Power control, Doubly-fed induction generator.

This paper presents a robust power control strategy using fractional order proportional-integral FO[PI] controller to enhance the performences of power control of a doubly fed induction generator (DFIG). In this paper, a new analytical design method is proposed and used to design FO[PI] controllers. The FO[PI] controllers designed in this way improve the control dynamics and robustness of the DFIG under various kinds of disturbances and parameters' variation. The originality of the present study lies in the development the new analytical design method, which is based on five frequency specifications, namely, phase margin, gain limitation at crossover frequency, robustness to gain variation, sensitivity and complementary sensitivity functions. The proposed method offers most of the advantages of the methods reported in the literature. Indeed, it guarantees robustness using phase margin, gain limitation and robustness to gain variation and disturbance rejection using sensitivity functions. Moreover, the complex analytical derivation is simplified using a change of variables and appropriate trigonometric formulas. The power control of the DFIG is examined with both integer order proportional integral controller IOPI, and fractional order proportional integral controller FO[PI]. The obtained results show that both IOPI and FO[PI] controllers give good performance under normal operation. However, FO[PI] controller fares better than IOPI controller under gain variation and various disturbances.

1. INTRODUCTION

The DFIG is the generator used by most of wind energy conversion systems (WECS) because of the control flexibility offered by this machine, and the reduced size of the power converters used [1–4]. The reliable operation of wind farms is highly dependent on the performances of the control strategy and the efficiency of the controllers used to achieve control objectives.

DFIG control strategies, which have been widely studied, range from vector control and direct power control to some forms of adaptive and variable structure control [4–7]. The most reported control strategy is the power control based on field-oriented control (FOC), in which independent control of active and reactive powers is achieved through the rotor side converter of the DFIG [1, 2, 4]. Classical controllers are very sensitive to variations over time in system parameters, and also to external disturbances [6], which may affect control objectives and system performance.

In recent years, a new form of controllers based on fractional order derivative and integral was proposed. Its synthesis and applications in physics and control engineering appeared at the end of the 20th century [7, 8]. The fractional order proportional and integral controller (FOPI) and the fractional order [proportional and integral] FO[PI] controller are a generalized form of the conventional integer order PI controller, which offers more flexibility in achieving control objectives [9]. Indeed, PI controllers have two parameters, namely k_p and k_i adjusted to obtain control objectives. However, FOPI and FO[PI] controllers have an additional parameter, namely the fractional integration order λ [10–13].

The major challenge in fractional order control resides in the design and analytical calculation of fractional order derivatives and integrals [7–11]. One viable alternative in analytic calculation is the integer order approximation discussed in [7, 8, 14]. For the design of fractional order (FO) controllers, several techniques have been studied in the literature, among which auto-tuning technique [15, 16], particle swarm optimization (PSO) [17], analytic tuning method using Bode's ideal transfer function [11], and analytical design method [16–18]. Other researchers used analytic design methods based on frequency domain specifications like A. Monje [16], H. Mahvash in [18] and Y. Q. Chen [19, 20].

The analytic design studies have been made based on both frequency domain specifications and time domain specifications. Nevertheless, it should be noted that analytical design methods based on time domain specifications are still insufficiently investigated in the literature and has still many difficulties.

However, several analytic design methods in frequency domain have been discussed. We can find the analytical design method proposed by H. Mahvash in [18] based on three frequency specifications, which are phase margin, gain limitation at the crossover frequency and robustness to gain variation. Where, at a given crossover frequency ω_c, robustness to plant uncertainties and overshoots limitation are guaranteed. However, this method involves a very complex analytical calculation that leads to nonlinear, coupled equations, which must be solved in order to determine the controller parameters. This technique was also applied by H. Mahvash [18] using complex analytical calculations. B. Boudjehem proposed in [21] an analytic method with only two frequency specifications; phase margin and gain margin. The common advantage of these methods is to achieve robustness to plant uncertainties and parameters variation. However, controllers designed in this way are not suitable for systems subject to external

[1] National Polytechnic School, Algiers, LRE Research Lab, Algeria, E-mail: metatla.samir@gmail.com
[2] University Larbi Tebessi, LABGET Research Lab, Tebessa, Algeria, E-mail: s.metatla@univ-tebessa.dz
[3] Ecole Normale Supérieure de Kouba, LSIC Research Lab, Algiers, Algeria, E-mail: ali.nesba@gmail.com
[4] Nisantasi University, Faculty of Engineering and Architecture, Istanbul, Turkey, E-mail: ilhcol@gmail.com
[5] High School of Applied Sciences of Algiers, Algeria, E-mail: ouadah@gmail.com

disturbances such as those due to load variations.

Another analytic design method was proposed by Y.Q. Chen in [19] based on sensitivity function and complementary sensitivity function specifications to satisfy the major industry design requirements, which are robustness to load disturbances and noise rejection [19]. On the other hand, this method is not effective in ensuring the robustness against plant uncertainties and parameters variation. The analytical design methods mentioned above require complex calculations and do not meet the requirements of modern control techniques

The originality of this paper consists of developing a new analytic design method based on five frequency specifications, which are phase margin, gain limitation at crossover frequency, robustness to gain variation, sensitivity function and complementary sensitivity function. The proposed method offers all the advantages of the methods cited above. So, it guarantees robustness using phase margin, gain limitation and robustness to gain variation and disturbance rejection using sensitivity functions. Moreover, the complex analytical derivation involved in [18] is simplified using a change of variables and appropriate trigonometric formulas.

This paper is organized as follows: in the subsequent section, a short review of the fractional calculus theory is presented including the advantages of using fractional controllers instead of integer order ones. The DFIG modeling and control are discussed in Section 3 with a detailed independent power control strategy. In Section 4 the proposed analytic design method is developed based on five frequency domain specifications. Finally, in Section 5 The performances of IOPI and FO[PI] controllers are discussed and compared.

2. **FRACTIONAL CALCULUS**

Fractional calculus was introduced in 1695 by the mathematician G.W Leibniz. Within years fractional calculation became an attractive subject to mathematicians as Liouville, Riemann and Holmgren [22].

Calculation of fractional derivatives and integrals is very difficult using analytical methods [22]. For simulation and Hardware implementation of fraction order transfer functions, an integer order approximation is usually employed [9]. In literature, two popular integer order recursive approximations can be found, Oustaloup's method [7–10, 23] and Charef's method [11–13]. Both, methods use a recursive distribution of poles and zeroes as given in [7]:

$$s^{\alpha} \approx k \prod_{n=1}^{N} \frac{1+\left(s/\omega_{z,n}\right)}{1+\left(s/\omega_{p,n}\right)}, \tag{1}$$

where:

$\omega_{z,1} = \omega_l . \sqrt{\eta}$;

$\omega_{p,1} = \varepsilon . \omega_{z,1}$; $\omega_{p,n+1} = \omega_{p,n} . \eta$; $n = 1, \ldots, (N-1)$;

$\eta = \left(\omega_h / \omega_l\right)^{(1-\alpha)/N}$; $\varepsilon = \left(\omega_h / \omega_l\right)^{\alpha / N}$.

This approximation is valid in the frequency range $[\omega_l, \omega_h]$. Gain k is calculated so that both sides of equation (1) shall have unit gain at 1 rad/s.

Fractional controllers are increasingly used in industry. The efficiency and robustness of this type of controllers makes them a good alternative to classical controllers such as PI and PID. In fact, fractional order proportional and integral controller FO[PI] is a generalization of the IOPI controller. It offers a space of three degrees of freedom instead of two for IOPI controller [8–14]. The transfer function of such controller can be expressed as:

$$C(s) = \frac{Y(s)}{X(s)} = \left(k_p + \frac{k_i}{s}\right)^{\lambda}, \tag{2}$$

where k_p is the proportional gain, k_i is the integral gain of the controller and λ is the integration order.

3. **DFIG MODELLING AND CONTROL**

The DFIG based WECS configuration is shown in Fig. 1. The generator stator windings are directly connected to the grid while the rotor ones are connected to the grid through two back-to-back converters, called the rotor side converter (RSC), and the grid side converter (GSC).

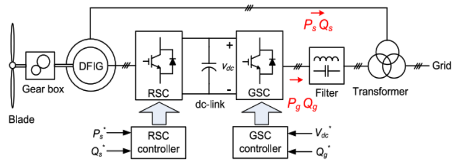

Fig. 1 – Typical configuration of the DFIG based wind energy conversion system

3.1. DFIG MODELING

The DFIG modeling is widely discussed in the literature [4, 7, 24–27]. The DFIG voltage equations in arbitrary rotating reference frame are given by :

$$\begin{cases} V_{dqs} = R_s I_{dqs} + \dfrac{\mathrm{d}}{\mathrm{d}t}\phi_{dqs} \mp \omega_s . \phi_{dqs} \\ V_{dqr} = R_r I_{dqr} + \dfrac{\mathrm{d}}{\mathrm{d}t}\phi_{dqr} \mp \omega_{sr} . \phi_{dqr} \end{cases}, \tag{3}$$

with $\omega_{sr} = \omega_s - \omega$ – rotor pulsation; ω_s, ω – synchronous speed and rotor speed, respectively; V_{dqs} and V_{dqr} – stator and rotor voltages along d and q axis, respectively; I_{dqs} and I_{dqr} – stator and rotor currents along d and q axes respectively; ϕ_{dqs} and ϕ_{dqr} – stator and rotor flux density along d and q axis, respectively; R_s and R_r – stator and rotor resistance, respectively.

The flux equations are by [28, 29]:

$$\begin{cases} \phi_{dqs} = L_s I_{dqs} + M . I_{dqr} \\ \phi_{dqr} = L_r I_{dqr} + M . I_{dqs} \end{cases}, \tag{4}$$

where L_s, L_r and M : stator inductance, rotor inductance and mutual inductance, respectively.

3.2. POWER CONTROL OF DFIG

To achieve power control of the DFIG, field-oriented control FOC technique is used. It consists in orienting the stator flux along d-axis of the rotating frame, which implies that $\phi_{ds} = \phi_s$ and $\phi_{qs} = 0$.

$$\begin{cases} \phi_{ds} = \phi_s = L_s I_{ds} + M I_{dr} \Rightarrow I_{ds} = \dfrac{V_s}{\omega_s . L_s} - \dfrac{M}{L_s} I_{dr} \\ 0 = L_s I_{qs} + M I_{qr} \Rightarrow I_{qs} = \dfrac{M}{L_s} I_{qr} \end{cases}, \tag{5}$$

where:

ϕ_{ds} and ϕ_s – stator flux in d axis and stator flux;
I_{ds} and I_{dr} – stator and rotor current in d axis;
V_s and L_s – stator voltage and leakage inductance;
I_{qs} and I_{qr} – stator rotor currents in q axis.

Taking (3) and (5) into account and substituting the flux equations in the rotor voltage equations and then applying the Laplace transformation, the rotor voltages equations become [24–27]:

$$\begin{cases} V_{dr} = R_r I_{dr} + \sigma L_r s I_{dr} - \omega_{sr} \sigma L_r I_{qr} \\ V_{qr} = R_r I_{qr} + \sigma L_r s I_{qr} + \omega_{sr} \sigma L_r I_{dr} + \omega_{sr} \dfrac{M V_s}{\omega_s L_s} \end{cases}, \tag{6}$$

where:
V_{dr} and V_{qr} – rotor voltage in *d* and *q* axes;
R_r and L_r – rotor resistance and leakage inductance.

In addition, $\sigma = 1 - \left(M^2 / \left(L_r L_s\right)\right)$ is the dispersion coefficient and $s = \mathrm{j}\omega$ Laplace operator. The quantities $\omega_{sr} \sigma L_r I_{dr}$ and $\omega_{sr} \sigma L_r I_{qr}$ are the cross coupling between the rotor d and q axes.

We denote $V'_{dr} = V_{dr} + E_{qr}$ and $V'_{qr} = V_{qr} + E_{dr}$, where

$$\begin{cases} E_{dr} = -\omega_{sr} \sigma L_r I_{dr} - \omega_{sr} \dfrac{M V_s}{\omega_s L_s} \\ E_{qr} = \omega_{sr} \sigma L_r I_{qr} \end{cases}, \tag{7}$$

with E_{dr} and E_{qr} rotor – induced voltages in *d* and *q* axes.

So, we can write:

$$\begin{cases} V'_{dr} = R_r I_{dr} + \sigma L_r s I_{dr} \\ V'_{qr} = R_r I_{qr} + \sigma L_r s I_{qr} \end{cases}, \tag{8}$$

where V'_{dr} and V'_{qr} derivatives of rotor voltages in *d* and *q* axes.

From these equations, the transfer function of the direct and quadrature rotor axes can be deduced.

$$\begin{cases} \dfrac{I_{dr}}{V'_{dr}} = \dfrac{k}{1 + \sigma T s} \\ \dfrac{I_{qr}}{V'_{qr}} = \dfrac{k}{1 + \sigma T s} \end{cases}, \tag{9}$$

where *T* is the time constant and defined as $T = L_r / R_r$ and *k* is the constant value and defined as $k = 1/R_r$.

Under field-oriented control (FOC) conditions, the active and reactive powers can be written as in Eq. (10) [28, 29]:

$$\begin{cases} P_s = -\dfrac{M V_s}{L_s} I_{qr} \\ Q_s = \dfrac{V_s^2}{\omega_s L_s} - \dfrac{M V_s}{L_s} I_{dr} \end{cases}. \tag{10}$$

From (9) and (10), independent power control block diagram of the DFIG can be derived as described in Fig. 2. All cross-coupling terms between *d* and *q* axes and the disturbance terms are being fully compensated.

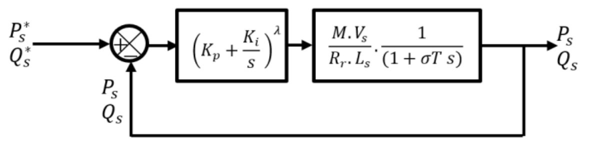

Fig. 2 – Power control block diagram of the DFIG using FO[PI] controller.

The power control block diagram illustrates the decoupled power control strategy using FO[PI] controllers in the rotating (d, q) reference frame according to the field oriented control of the DFIG [24–27].

4. **FO[PI] DESIGN METHODOLOGY**

4.1 FREQUENCY DOMAIN SPECIFICATIONS

Controllers design is a critical step in engineering industrial process control systems. Indeed, several design methods have been proposed by many contemporary researchers. A tuning methodology for fractional order controllers has been studied in [17, 19]. Time domain design of FOPI has been studied in [17] and frequency domain optimization tuning methods for fractional PI controllers have been proposed in [16, 23–25, 28]. The frequency domain design method is performed using frequency domain specifications as phase margin, gain limitation and robustness to the gain variation.

At a given crossover frequency ω_c, the analytic design method can be applied to DFIG power control system to design FO[PI] controllers using frequency domain specifications as follow:

– phase margin φ_m

$$\arg\left[plant + controller\right]_{\omega_c} = \varphi_m - \pi. \tag{11}$$

– robustness to gain variation

$$\frac{\mathrm{d}}{\mathrm{d}\,\omega} \left(\arg\left[plant + controller\right]\right)\Big|_{\omega_c} = 0. \tag{12}$$

– gain limitation

$$\left|plant + controller\right|\Big|_{\omega_c} = 1. \tag{13}$$

As it can be seen, the analytical method employs an open-loop transfer function at given crossover frequency, which may affect the control performance regarding closed loop stability, high frequency noise rejection and load disturbance rejection [16, 17].

To further enhance the robustness and performance of the DFIG power control, two sensitivity specifications are added. Therefore, the proposed design method uses five specifications to ensure control performance and robustness.

– Complementary sensitivity (noise rejection)

$$\left.\frac{\left(plant + controller\right)}{1 + \left(plant + controller\right)}\right|_{\omega} \le \left(1 - S\right) \quad \forall \omega \ge \omega_h. \tag{14}$$

– Sensitivity (load disturbance rejection):

$$\left.\frac{1}{1 + \left(plant + controller\right)}\right|_{\omega} \le S \quad \forall \omega \le \omega_l, \tag{15}$$

where $\left[\omega_l, \omega_h\right]$ is the desired frequency range with $\omega_c \in \left[\omega_l, \omega_h\right]$ and S is the sensitivity value chosen to obtain a good performance. After the FO[PI] design is completed using equations (11), (12) and (13), the supplementary closed-loop specifications must be fulfilled. Otherwise, crossover frequency value ω_c should be chosen from the interval $\left[\omega_l, \omega_h\right]$ to satisfy supplementary specifications. So, the proposed FO[PI] design strategy can be outlined by the diagram bellow.

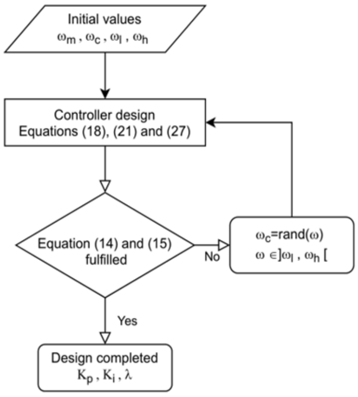

Fig. 3 – Proposed FO[PI] design strategy.

4.2. FO[PI] CONTROLLERS DESIGN

Considering the bloc diagram presented in Fig. 2, the power control transfer function can be expressed as:

$$H(s)=C(s)P(s)=\left(k_p+\frac{k_i}{s}\right)^{\lambda}\left(\frac{k}{1+\sigma Ts}\right), \tag{16}$$

where $C(s)$ and $P(s)$ are the controller and plant transfers functions respectively and $k=\dfrac{MV_s}{R_rL_s}$.

Applying the frequency domain specifications stated by (11), (12) and (13) on the system transfer function given by (16) and using analytical development, simplified relationships linking the FO[PI] controller parameters can be established as detailed in subsections bellow.

4.2.1 PHASE MARGIN φ_m

The phase margin is an important robustness measure. It can be also considered as a performance indicator because it is related to the system damping [16]. The phase margin equation is given by:

$$\arg[H(s)]=\arg\left[\left(k_p+\frac{k_i}{s}\right)^{\lambda}\left(\frac{k}{1+\sigma Ts}\right)\right]=\varphi_m-\pi .$$

At crossover frequency, we can write: $s=j\omega_c$

$$\arg[H(s)]=-\lambda\arctan\left(\frac{k_i}{k_p\omega_c}\right)-\arctan(\sigma T\omega_c)=\varphi_m-\pi$$

$$\Rightarrow \frac{k_i}{k_p.\omega_c}=\tan\left[\frac{\pi-\varphi_m-\arctan(\sigma T.\omega_c)}{\lambda}\right]. \tag{17}$$

By choosing $A=\left(\pi-\varphi_m-\arctan(\sigma T\omega_c)\right)$, a simple equation linking the controller parameters may be written as follows:

$$k_i=k_p.\omega_c\tan\left(\frac{A}{\lambda}\right). \tag{18}$$

4.2.2. ROBUSTNESS TO GAIN VARIATION

This specification is also called iso-damping property in time domain response. It ensures that the phase of the open-loop system is flat around the crossover frequency ω_c which means that the system is more robust to gain changes and the over shoot of the response is almost constant within a gain variation [16, 17].

$$\left.\frac{d(\arg[H(s)])}{d\omega}\right|_{\omega_c}=\lambda\frac{k_i/(k_p\omega_c^2)}{1+(k_i/k_p\omega_c)^2}-\frac{\sigma T}{1+(\sigma T\omega_c)^2}=0,$$

$$\Rightarrow \lambda\frac{k_i/(k_p\omega_c^2)}{1+(k_i/k_p\omega_c)^2}=B, \tag{19}$$

where $B=\dfrac{\sigma T}{1+(\sigma T\omega_c)^2}$.

4.2.3. GAIN LIMITATION

$$|H(j\omega)|_{\omega_c}=\left[(k_p)^2+\left(\frac{k_i}{\omega_c}\right)^2\right]^{\frac{\lambda}{2}}.\frac{k}{\left[1+(\sigma T\omega_c)^2\right]^{\frac{1}{2}}}=1,$$

$$\Rightarrow (k_p)^2+\left(\frac{k_i}{\omega_c}\right)^2=\left[\frac{\sigma T}{kB}\right]^{\frac{1}{\lambda}}. \tag{20}$$

By substituting (18) in (20), we find:

$$k_p=\left[\frac{\left[\sigma T/kB\right]^{\frac{1}{\lambda}}}{1+\tan^2\left(\frac{A}{\lambda}\right)}\right]^{\frac{1}{2}}. \tag{21}$$

The substitution of (18) in (19) leads to:

$$\frac{\lambda}{\omega_c}.\frac{\tan(A/\lambda)}{1+\tan^2(A/\lambda)}=B. \tag{22}$$

Equation (22) has the form of the well-known advanced trigonometric formula below.

$$\frac{2.\tan(\theta)}{1+\tan^2(\theta)}=\sin(2\theta). \tag{23}$$

Therefore, (22) may be written as:

$$\frac{\lambda}{\omega_c}.\frac{1}{2}\sin\left(2\frac{A}{\lambda}\right)=B. \tag{24}$$

Then we can write:

$$\frac{\sin(2A/\lambda)}{2A/\lambda}=\frac{B\omega_c}{A}. \tag{25}$$

This has the form of the well-known mathematical function called cardinal sinus defined by:

$$\mathrm{sinc}(\theta)=\frac{\sin(\theta)}{\theta},\quad \theta>0. \tag{26}$$

Finally, (25) can be written in a simpler form as:

$$sinc\left(2\frac{A}{\lambda}\right)=\frac{B\omega_c}{A}. \tag{27}$$

Equation (27) is a simple one variable equation, which can be resolved to obtain the fractional integration parameter λ. Then, the parameters k_p and k_i can be obtained by substituting the fractional integration parameter λ in (18) and (21), respectively.

According to the proposed design strategy shown by Fig.

3, the controller design steps (equations (18), (21) and (27)) should be repeated until the sensitivity specifications defined by (14) and (15) are fulfilled.

5. SIMULATION RESULTS AND DISCUSSION

In this section, simulation results are presented using FO[PI] controller and IOPI controller. Then, a comparison of power control performance between FO[PI] and IOPI under different operating conditions is achieved. The DFIG parameters variation, gain variation and robustness to grid disturbance are discussed. The design of the FO[PI] controllers is based on the analytic design method proposed in Subsection 4.1, considering phase margin $\varphi_m = 50°$ and a crossover frequency value $\omega_c = 100\,\text{rad/s}$. The DFIG parameters are given in Table 1 below.

Table 1

DFIG parameters

Parameter	Value
Rated power	300 kW
Rated voltage	690 V
Stator resistance	0.0063 Ω
Rotor resistance	0.003 Ω
Stator inductance	0.0118 H
Rotor inductance	0.0115 H
Magnetizing inductance	0.0115 H
Rated stator frequency	50 Hz
Number of pole pairs	2

The FO[PI] parameters obtained from (18), (21) and (27) are: $\lambda = 0.588$, $k_i = 786.3$, $k_p = 1844$.

5.1. REFERENCE TRACKING TESTS

The DFIG is supposed to be operated at 1500 rpm when different input steps for active and reactive powers are applied. The dynamic performances of both FO[PI] and IOPI controllers are depicted in Figs. 4 – 8 below.

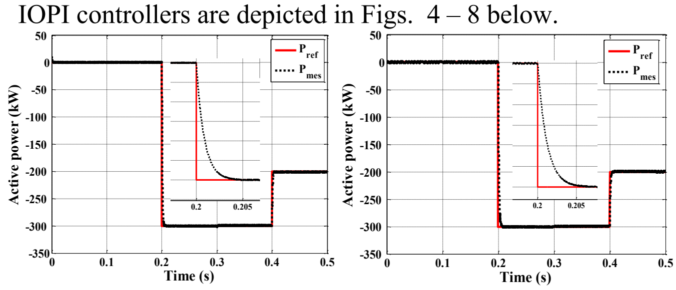

(a) FO[PI] controller (b) IOPI controller

Fig. 4 – Dynamic response to active power steps.

Simulation results show that both FO[PI] and IOPI controllers give a good reference tracking in a short response time without static error.

5.2. ROBUSTNESS TESTS

The robustness tests are performed under DFIG parameter variations as follows:

– the first test: the rotor resistance value is increased by 70 % from its nominal value;
– the second test: the stator inductance is increased by 20 % from its nominal value;
– the third test: both rotor resistance and stator inductance are changed simultaneously.

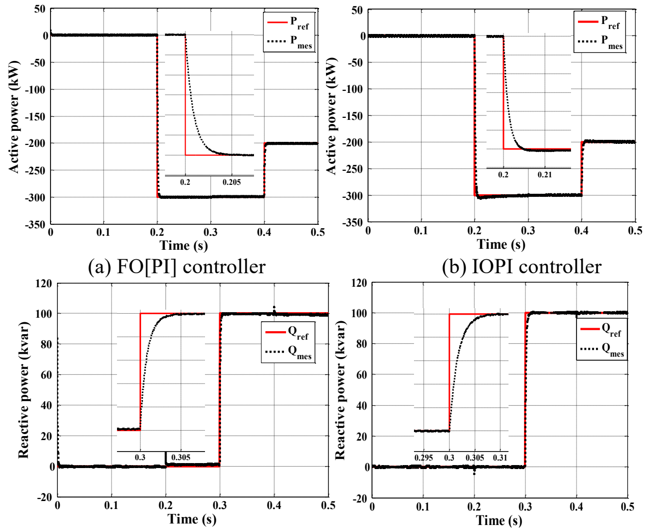

(a) FO[PI] controller (b) IOPI controller

(c) FO[PI] controller (d) IOPI controller

Fig. 5 – Power control robustness against R_r variation.

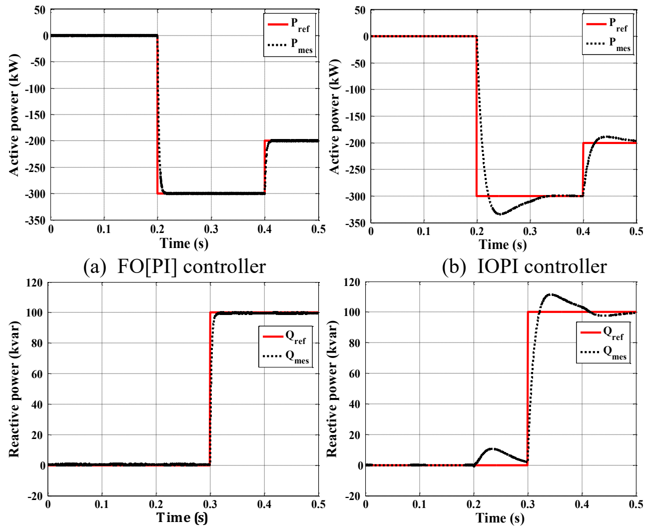

(a) FO[PI] controller (b) IOPI controller

(c) FO[PI] controller (d) IOPI controller

Fig. 6 – Power control robustness against L_s variation.

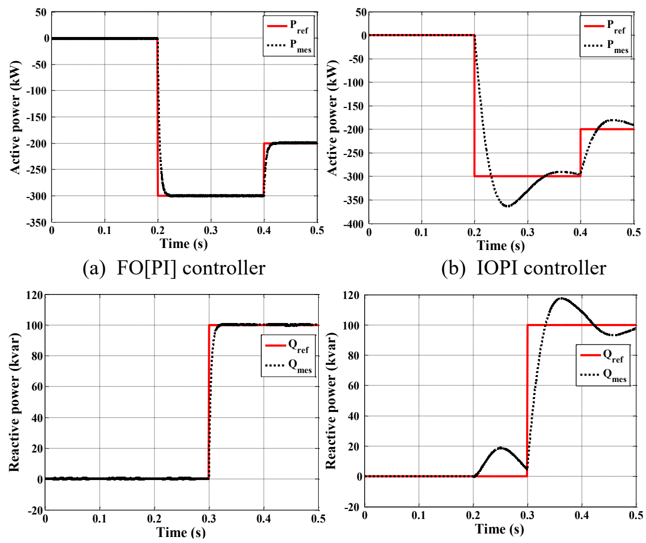

(a) FO[PI] controller (b) IOPI controller

(c) FO[PI] controller (d) IOPI controller

Fig. 7 – Power control robustness against simultaneous R_r and L_s variation.

Figures 5, 6, and 7 show the parameters variation effect on active and reactive power response for FO[PI] and IOPI controllers. As we can see from Fig. 5 for both controllers, rotor resistance variation does not have a significant effect on control performance. However, stator inductance L_s variation has a significant impact on system performance, particularly for the IOPI controller, which can affect system stability. On the other hand, by using FO[PI], the system stability is guaranteed even with parameters variation as can be seen in Figs. 6 and 7. So, we can easily conclude from the robustness test that the FO[PI] controller is more efficient than the IOPI one.

As described in Subsections 4.1 and 4.2, the FO[PI] controller is designed to be robust against gain variations using frequency specification given by (12). This property can be observed when varying the system parameters or the proportional coefficient of FO[PI] controllers.

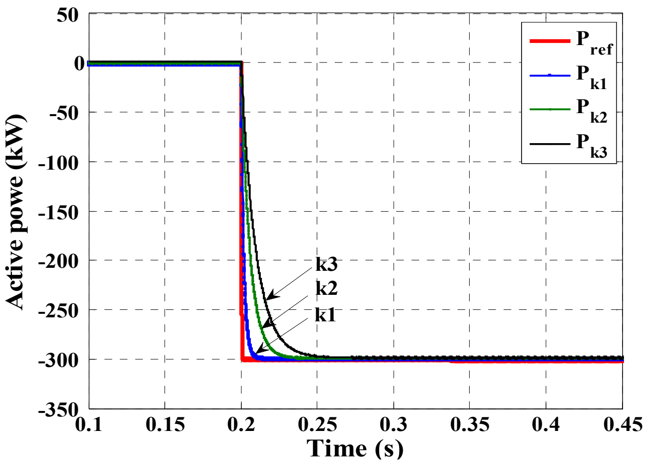

Fig. 8 – FO[PI] gain variation robustness.

Figure 8 shows active power control robustness against gain variation. The robustness test to gain variation agrees with the studies performed by H. Mahvash in [18], CA. Monje in [19] and B. Boudjehem in [21].

6. CONCLUSION

The idea of this paper is to design of FO[PI] controllers by using frequency domain specifications and its application in the power control of DFIG. First, the decoupled power control strategy of DFIG is established. The FO[PI] analytical design approach detailed in [18] is simplified using advanced trigonometric formulas and applied to the power control of DFIG. A comparative study of power control using IOPI and FO[PI] controllers is discussed based on various tests.

Robustness tests against plant parameters variation and gain variation show that, with FO[PI], the system stability is achieved under various disturbances such as load variation and gain variation for which peak overshoots for different gain values are the same as it can be observed on Fig. 8. However, with IOPI, peak overshoots and stability are strongly affected by the gain variation.

In light of these results, it can be concluded that the FO[PI] controller is more efficient than the IOPI controller, particularly for the stability and robustness of the system.

Received on November 13, 2018

REFERENCES

1. R. Bhattarai, N. Gurunget, A. Thakallapelli, S. Kamalasadan, *Reduced Order State Observer Based Feedback control methodologies for Doubly Fed Induction machine*, IEEE Transactions on Industry Applications, **54**, *3*, pp. 2845 – 2856 (2018).
2. W. Yuan-Kang, W-H Yang, *Different control strategies on the rotor side converter in DFIG based wind turbines*, Energy Procedia, **100**, pp. 551–555 (2016).
3. L. Xu, P. Cartwright, *Direct active and reactive power control of DFIG for wind energy generation*, IEEE Transactions on Energy Conversion, **21**, *3*, pp. 750–758 (2006).
4. R. Cardenas, R. Pena, S. Alepuz, G. Asher, *Overview of Control Systems for the Operation of DFIGs in Wind Energy Applications*, IEEE Transaction on industrial electronics, **60**, *7*, pp. 2776–2798 (2013)
5. M. Rahimi, M. Parniani, *Dynamic behavior analysis of doubly-fed induction generator wind turbines – The influence of rotor and speed controller parameters*, Electrical Power and Energy Systems, **32**, *5*, pp. 464–477 (2010).
6. O. Bachir, A-F, Zoubir, *Comparative analysis of robust controller based on classical proportional-integral controller approach for power control of wind energy system*, Rev. Roum. Sci. Techn.– Electrotechn. et Energ., **63**, *2*, pp. 210–216 (2018).
7. A. Oustaloup, F. Levron, B. Mathieu, F. M. Nanot, *Frequency-Band Complex Noninteger Differentiator: Characterization and Synthesis*, IEEE Transaction on circuits and systems –I: Fundamental theory and applications, **47**, *1*, pp. 25–39 (2000).
8. A. Oustaloup, *Systèmes Asservis Linéaires d'Ordre Fractionnaire: Théorie et Pratique*, Masson, Paris, France, 1983, pp. 50–150.
9. M. Zamani, M. K. Ghartemani, N. Sadati, *FOPID controller design for robust performance using particle swarm optimization*, Fractional calculus and applied analysis, **10**, *2*, pp. 169-187 (2007).
10. I. Podlubny, *Fractional-Order Systems and $PI^{\lambda}D^{\mu}$ Controllers*, IEEE Transaction on automatic control, **44**, *1*, pp. 208–214 (2000).
11. A. Djouambi, A. Charef, A.V. Besanc, *Fractional order controllers based on Bode's ideal transfer function*, International Journal of Control and Intelligent Systems, **38**, *2*, pp 67–73 (2010).
12. N. Fergani, A. Charef, *Process step response based fractional $PI^{\lambda}D^{\mu}$ controller parameters tuning for desired closed loop response*, International Journal of Systems Science, **47**, *3*, pp. 521–532 (2015).
13. A. Beddar, H. Bouzekri, B. Babes, H. Afghoul, *Real time implementation of improved fractional order proportional-integral controller for grid connected wind energy conversion system*, Rev. Roum. Sci. Techn.– Electrotechn. et Energ., **61**, *4*, pp. 402–407 (2016).
14. K. Bettou, A. Charef, *Control quality enhancement using fractional PIλDμ controller*, International Journal of Systems Science, **40**, *8*, pp. 875–888 (2009).
15. R.D. Keyser, C.I. Muresan, C.M. Ionescu. *A novel auto-tuning method for fractional order PI/PD controllers*, ISA Transactions, **62**, *3*, pp. 68–75 (2016).
16. A. Monje, B. M. Vinagre, V. Feliu, Y. Q. Chen, *Tuning and auto-tuning of fractional order controllersfor industry applications*, Control Engineering Practice **16**, 7, pp. 798–812 (2008).
17. S. Das, S. Saha, Sh. Das, A. Gupta, *On the selection of tuning methodology of FOPID controllers for the control of higher order processes*, ISA Transactions, **50**, *3*, pp. 376–388 (2011).
18. H. Mahvash, S. A. Taher, M. Rahimi, M. Shahidehpour, *DFIG performance improvement in grid connected mode by using fractional order [PI] controller*, Electrical Power and Energy Systems, **96**, *3*, pp. 398–411 (2018).
19. CA. Monje, AJ. Calderon, BM. Vingre, YQ. Chen, V. Feliu, *On fractional PI^{λ}controllers: some tuning rules for robustness to plant uncertainties*, Nonlinear Dynamics, **38**, *2*, pp. 69–81 (2004).
20. Y.Q. Chen, T. Bhaskaran, D. Xue, *Practical tuning rule development for fractional order proportional and integral controllers*, Journal of Computational and Nonlinear Dynamics, **03**, *2*, pp. 1–8 (2008).
21. B. Boudjehem, D. Boudjehem, H. Tebbikh, *Analytical design method for fractional order controller using fractional reference model* New Trends in Nanotechnology and Fractional Calculus Applications, 2009, pp. 295–303.
22. A.B. Malinowska *et al.*, *Advanced Methods in the Fractional Calculus of Variations*, Springer Briefs in Applied Sciences and Technology, 2015, pp. 31–82.
23. D. Abdelhamid, T. Bouden, A. Boulkroune, *Design of a fractional order PID controller (FOPID) for a class of fractional order*

MIMO systems, J. Automation & Systems Engineering **8**, *1*, pp. 25–39 (2014).
24. A. Boyette, S. Saadate, P. Poure, *Direct and indirect control of a Doubly Fed Induction Generator wind turbine including a storage unit*, IEEE Industrial Electronics, 2006, pp. 2517–2522.
25. M. Adjoudj, M. Abid, A. Aissaoui, Y. Ramdani, H. Bounoua, *Sliding mode control of a doubly fed induction generator for wind turbines*, Rev. Roum. Sci. Techn. – Electrotechn. et Energ., **56**, *1*, pp. 15–24 (2011).
26. S. Metatla, S. Mekhtoub, R. Ibtiouen, A. Nesba, *Dynamic behavior of doubly fed induction generator during network voltage dips*, ICET in Maghreb, 2014, pp. 1–6, Morocco.
27. B. K. Bose, *Power Electronics and AC Drives*, Englewood Cliffs, N. J. Prentice-Hall, New York, 1986.
28. I. Kharchouf, A. Essadki, T. Nasser, *Wind System Based on a Doubly Fed Induction Generator: Contribution to the Study of Electrical Energy Quality and Continuity of Service in the Voltage Dips Event*, International journal of renewable energy research, **7**, *4*, pp. 1892–1900 (2017).
29. B. Hamane, M. L. Doumbia, M. Bouhamida, A. Draou, H. Chaoui, M. Benghanem, Comparative Study of PI, RST, *Sliding Mode and Fuzzy Supervisory Controllers for DFIG based Wind Energy Conversion System*, International journal of renewable energy research, **5**, *4*, pp. 1174–1185 (2015).
30. B. Benlahbib**,** N.Bouarroudj, F. Ouchafaa, B. Batoun, *Fractional Order PI Controller for Wind Farm Supervision,* IEEM, 2014, pp. 1234–1238.